The 22nd Lomonosov Conference on Elementary Particle Physics

JINR

Joint Institute for Nuclear Research

Lomonosov Moscow State University

# Amplitude analysis of dicharmonium resonances

Ivan Yeletskikh, Leonid Gladilin, Alisa Didenko

21 – 27 of August 2025

# The firs experimental observation on LHCb

[1] Observation of structure in the J/ψ-pair mass spectrum [arXiv:2006.16957v2]

model I

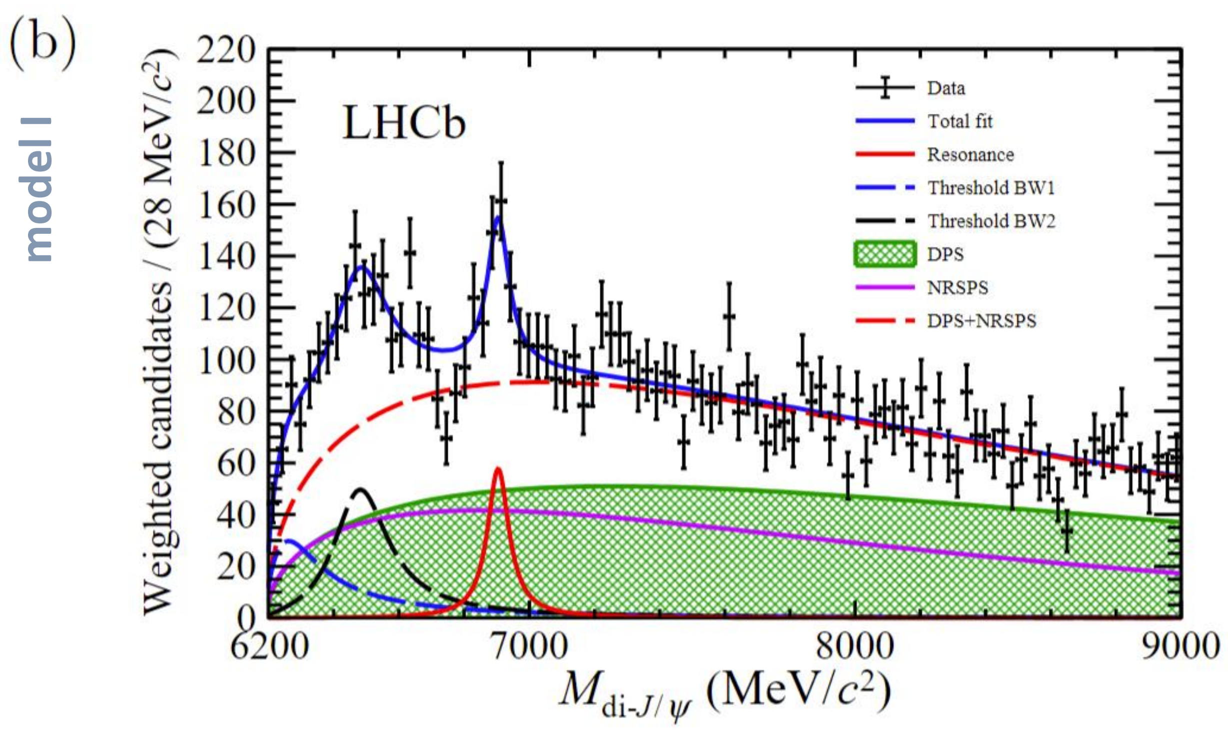


model II

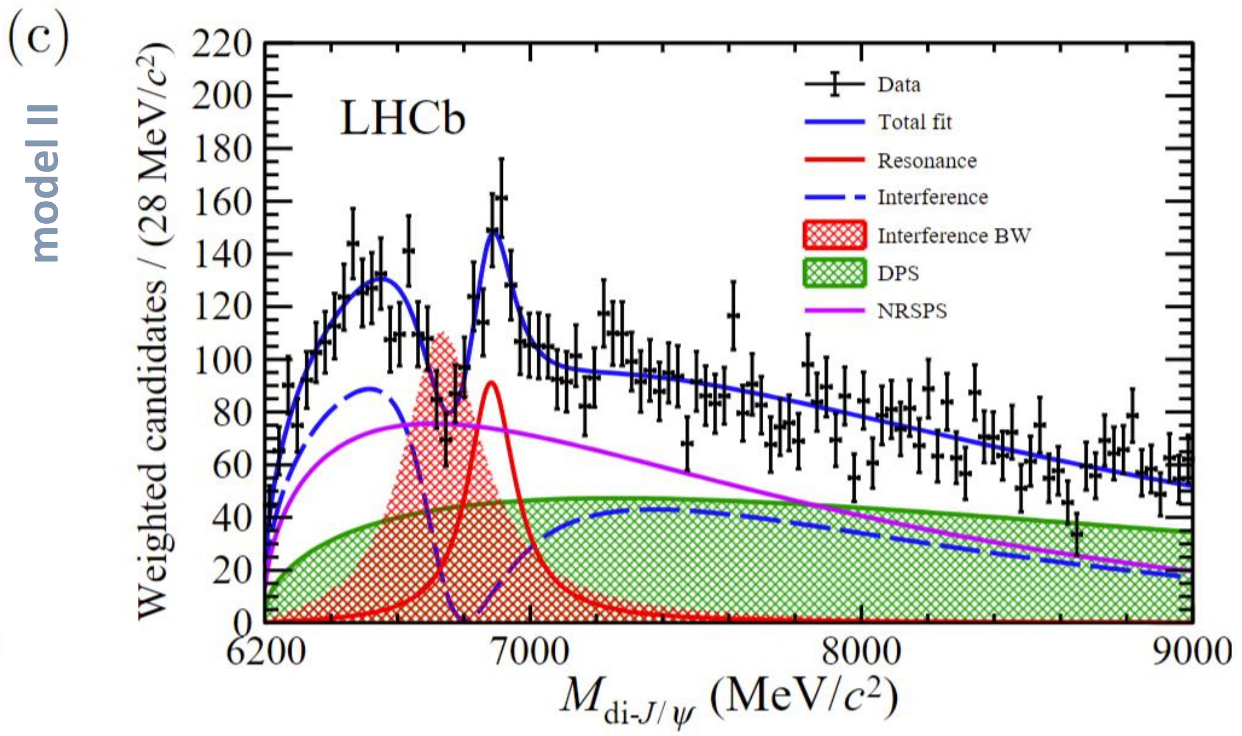


- **Model I**: the addition of 3 resonant components
- **Model II**: interference between the near-threshold structure with the non-resonant SPS and noninterfering resonance at 6900.

The $\chi^2$ test statistic of the model I corresponding to a probability of 4.6%. The model II has a probability of 15.5%.

| X(6900) | No-interference, I LHCb | Interference, II LHCb |
|---|---|---|
| m, GeV | 6.905 | 6.886 |
| Γ, GeV | 0.080 | 0.168 |

# The latest experimental observation. ATLAS

[2] Observation of an excess of di-charmonium events in the four-muon final state with the ATLAS detector [arXiv:2304.08962v2]

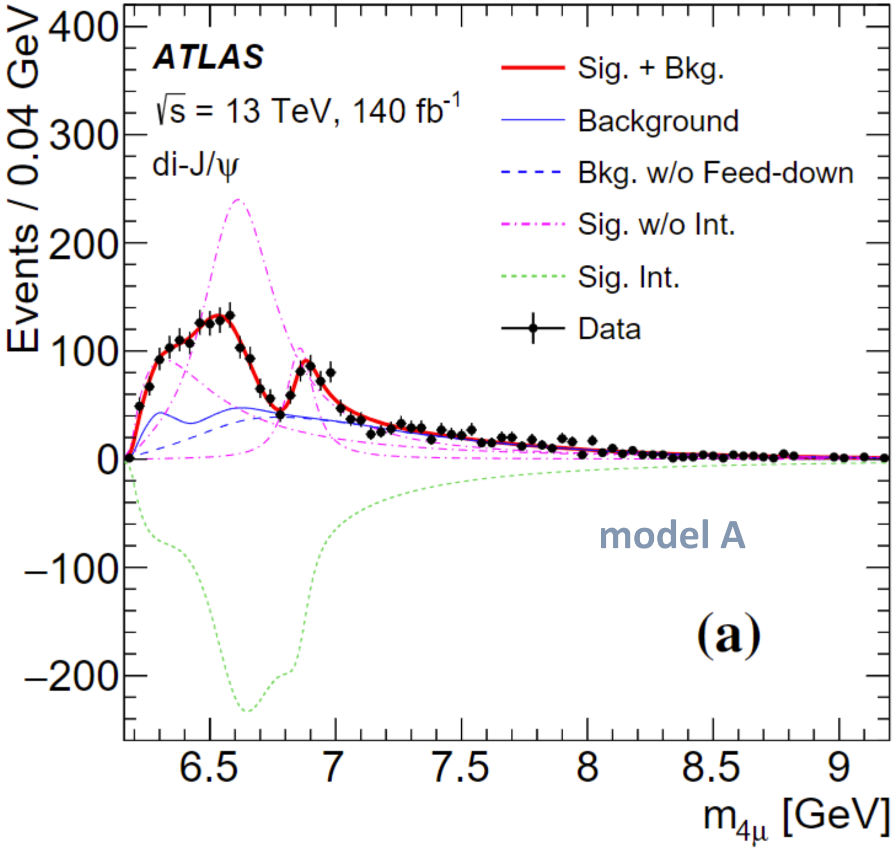


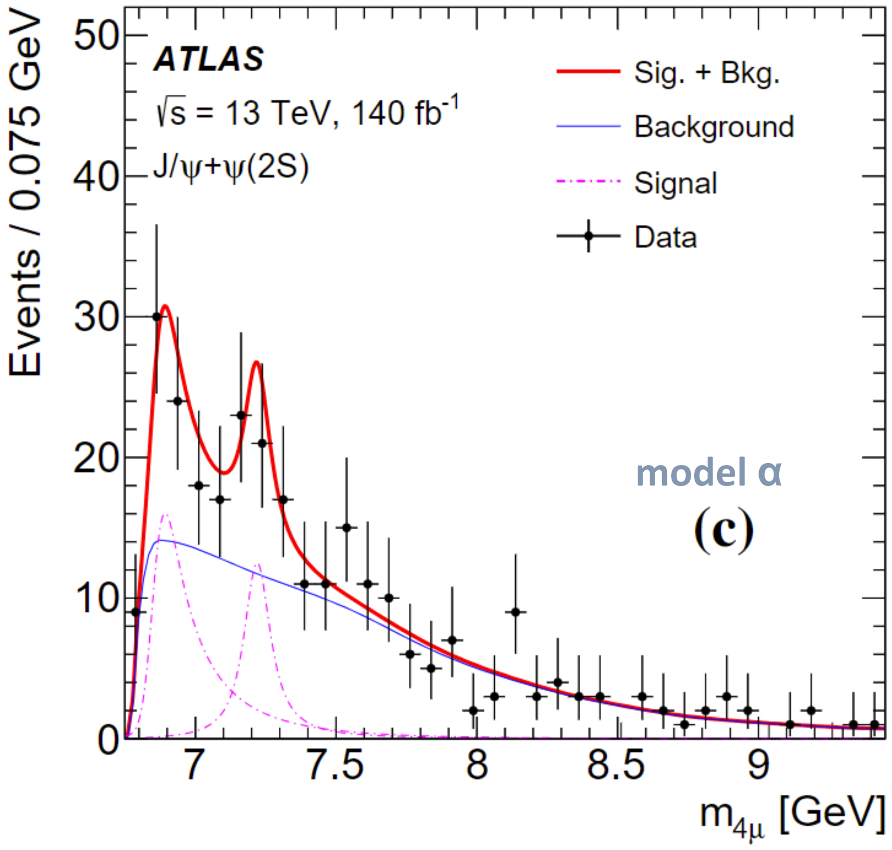


- **Model A**: interference of three states with each other;
- **Model α**: mass at 6.9 is fixed on model A, and the state at 7.2 is added without interference.

The mass of the third resonance, $m2$, is consistent with the LHCb mass.

| | | $BW_0$ | $BW_1$ | $BW_2$ | | $BW_3$ |
|---|---|---|---|---|---|---|
| model A | m, GeV | 6.41 | 6.63 | 6.86 | model α | 7.22 |
| | Γ, GeV | 0.59 | 0.35 | 0.11 | | 0.09 |

# The latest experimental observation. CMS

[6] CERN LHC Seminar: Symmetry properties of all-charm tetraquarks with CMS (8 April 2025) [https://indico.cern.ch/event/1533044/]

## CMS Run 2 for J/ψJ/ψ channel

[3] New Structures in the J/ψJ/ψ Mass Spectrum in Proton-Proton Collisions at √s = 13 TeV [arXiv:2306.07164v2]

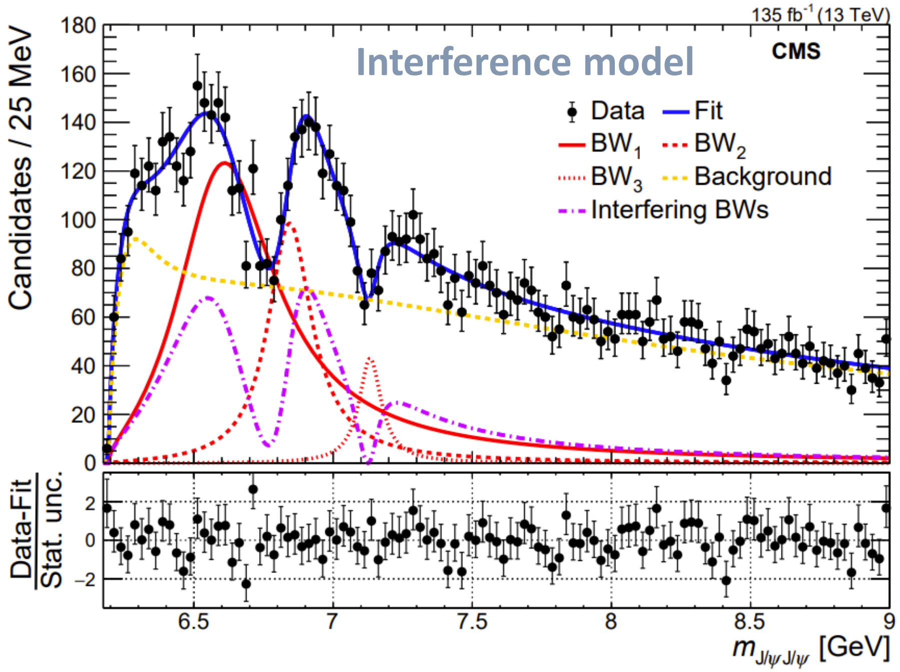


[8] Spin and symmetry properties of all-charm tetraquarks

**The Matrix Element Likelihood Analysis (MELA)** using kinematic discriminant: $\mathbf{J^{PC} = 2^{++}}$ quantum numbers is favored. The spin J of X(6900) exoticstates is most consistent with J=2h, a value that is uncommon for such particles, while the J=0h and J=1h are excluded at 95% and 99% confidence level, respectively.

## CMS Run 2 + Run 3 for J/ψψ(2S) channel

[7] Observation of X(6900) and evidence of X(7100) in the psi(2S)Jpsi to 4mu mass spectrum in pp collisions at CMS

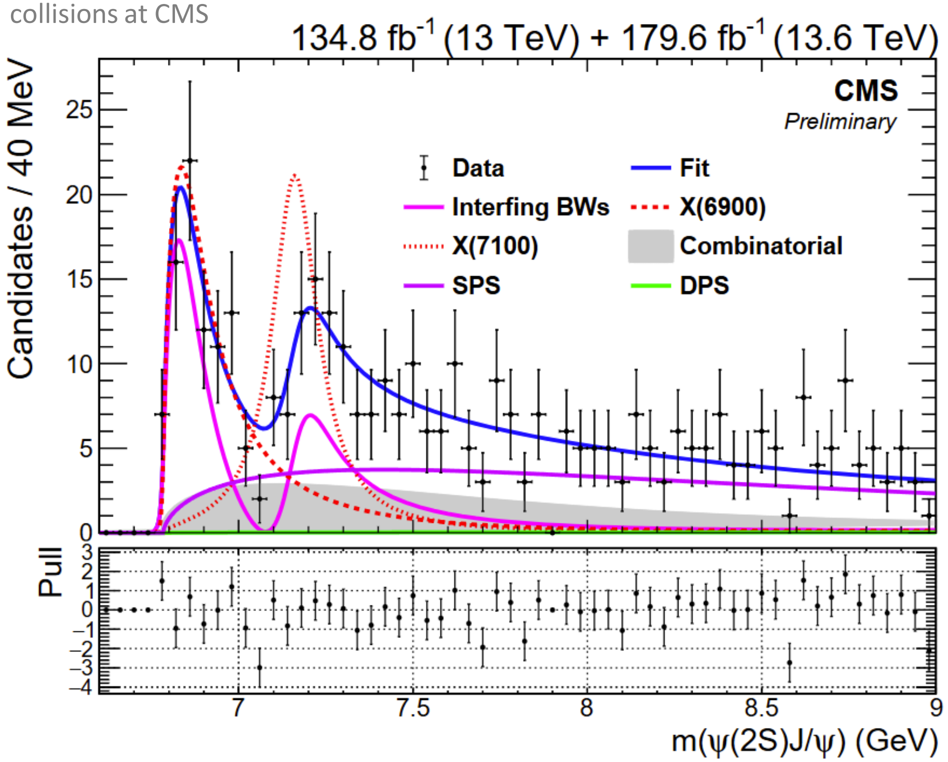


| | J/ψJ/ψ Run 2 (CMS) | | J/ψψ(2S) Run 2 + Run 3 (CMS) | |
|---|---|---|---|---|
| | m, GeV | Γ, GeV | m, GeV | Γ, GeV |
| $BW_1$ | 6.638 | 0.440 | -- | -- |
| $BW_2$ | 6.847 | 0.191 | 6.876 | 0.253 |
| $BW_3$ | 7.134 | 0.097 | 7.169 | 0.154 |

# The latest experimental observation. Amplitude analysis by CMS

[6] CERN LHC Seminar: Symmetry properties of all-charm tetraquarks with CMS (8 April 2025) [https://indico.cern.ch/event/1533044/]

## CMS Run 2 for J/ψJ/ψ channel

[8] Spin and symmetry properties of all-charm tetraquarks

**The Matrix Element Likelihood Analysis (MELA)** using kinematic discriminant: **$J^{PC} = 2^{++}$** quantum numbers is favored.

The spin J of X(6900) exoticstates is most consistent with J=2h, a value that is uncommon for such particles, while the J=0h and J=1h are excluded at 95% and 99% confidence level, respectively.

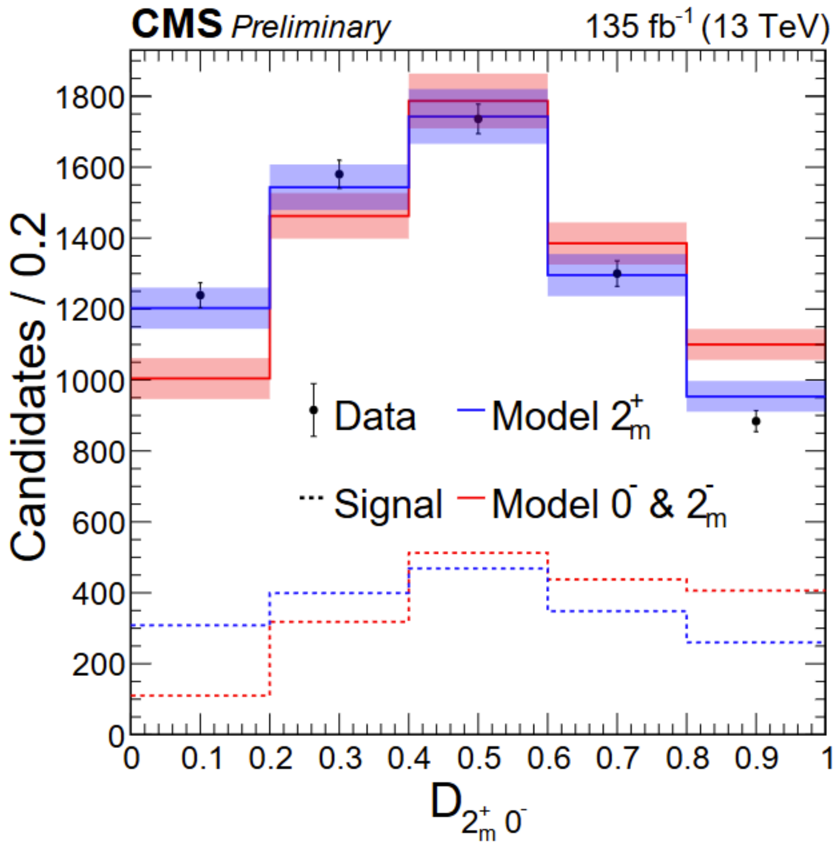


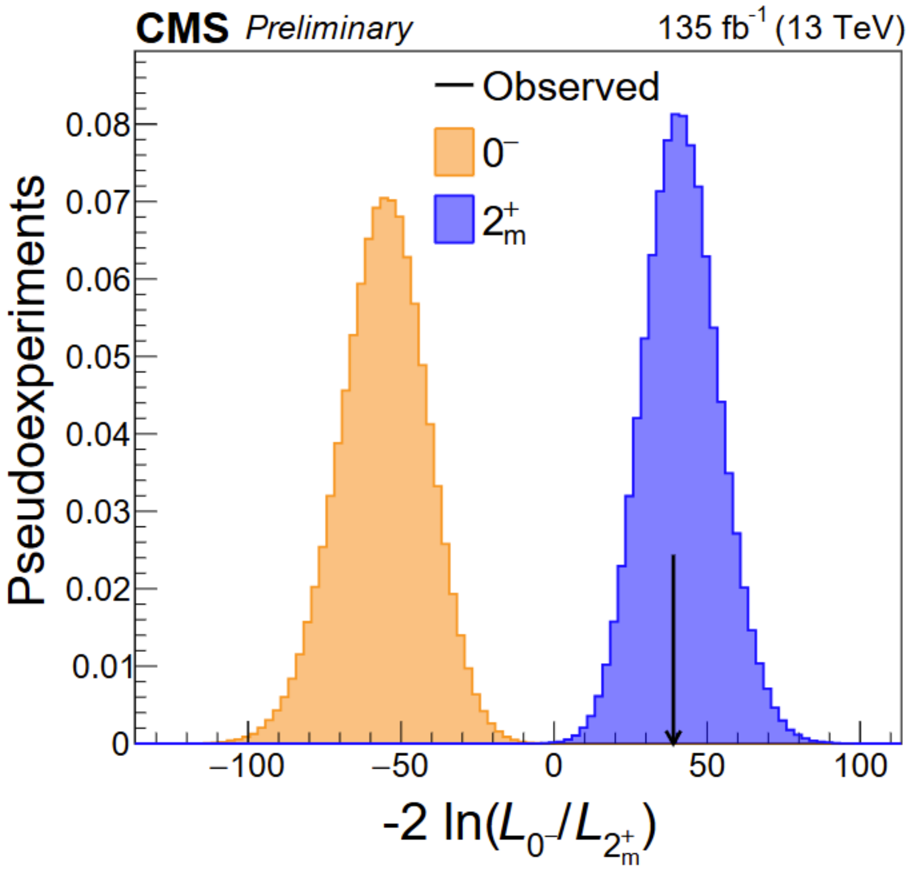


| $J_X^P$ | p-value | Z-score reject $J_X^P$ |
|---|---|---|
| $0^-$ | $2.7 \times 10^{-13}$ | 7.2 |
| $0_m^+$ | $4.3 \times 10^{-5}$ | 3.9 |
| $0_{mix}^+$ | $1.4 \times 10^{-2}$ | 2.2 |
| $0_h^+$ | $3.1 \times 10^{-9}$ | 5.8 |
| $1^-$ | $8.0 \times 10^{-8}$ | 5.2 |
| $1^+$ | $4.7 \times 10^{-3}$ | 2.6 |
| $2_m^-$ | $4.1 \times 10^{-12}$ | 6.8 |
| $2_{mix}^-$ | $6.5 \times 10^{-4}$ | 3.2 |
| $2_h^-$ | $2.2 \times 10^{-8}$ | 5.5 |

# $T_{cc\bar{c}\bar{c}}$ production mechanism

The narrow resonant-like structures were discovered by three main LHC collaborations in the di-Jpsi, Jpsi-Psi2S invariant mass spectra suggesting existence of the fully-heavy tetraquarks with a $cc\bar{c}\bar{c}$ configuration.

- 2019-2020: **X(6900)** by LHCb [1]
- 2023: **X(6500), X(6600), X(6900), X(7200)** by ATLAS [2]
- 2024: **X(6500), X(6600), X(6900)** by CMS [3]

[4] On the mechanism of T4c(6900) tetraquark production [arXiv:2009.02100v1]

- Different bound state structures suggest the possibility of different production mechanisms, for example via the DPS mechanism.
- Pt signal spectrum is sensitive to the mechanism of $T_{cc\bar{c}\bar{c}}$ production.

SPS

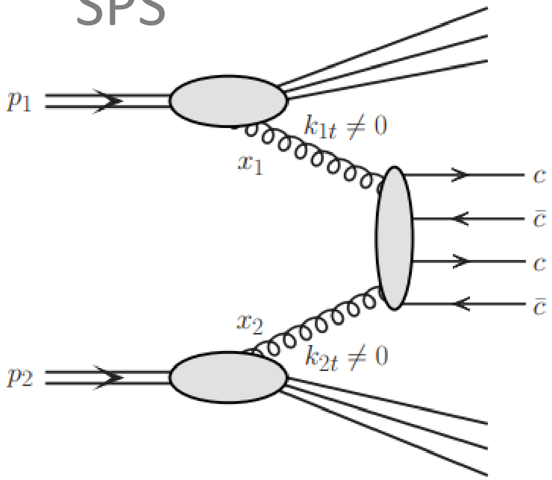


DPS

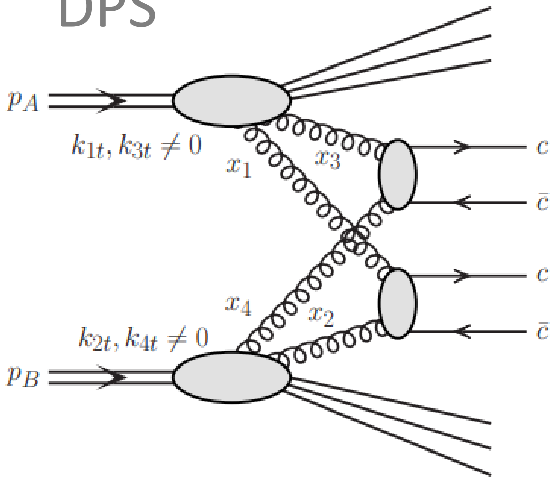


gg fusion

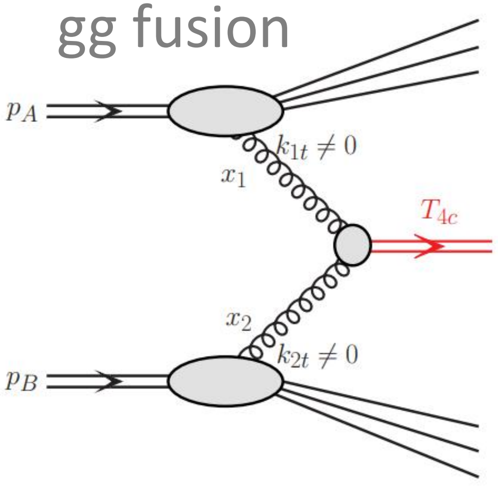


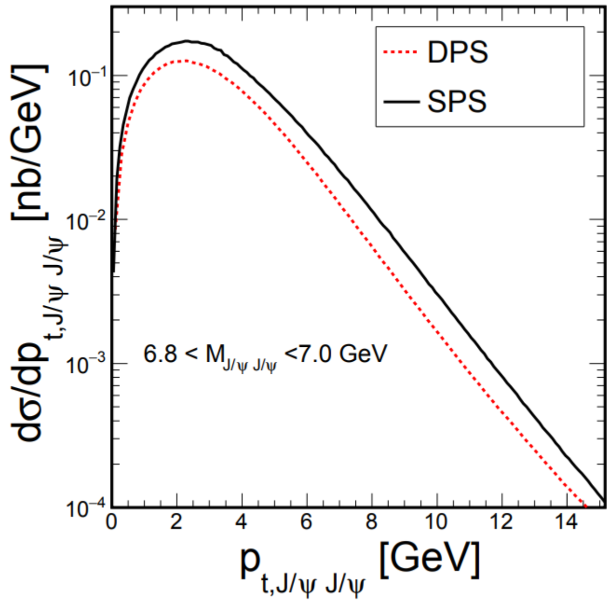

# Predictions of theoretical models

## Compact tetraquark

Tetraquark models may be composed of the confinement potential plus 'color' interactions

One-gluon-exchange interaction + non-relativistic confinement potential [6].

- Radial excitations of the S-wave tetraquarks Blue and Red spectra correspond to different model parameters.
- Masses of signals (depending on model parameters) agree with experimental values.
- States at **6405, 6498, 6867** and **7007** are predicted for **0++**

[9] Higher fully-charmed tetraquarks: Radial excitations and P-wave states [arXiv:2105.13109]

| | $J^{PC}$ | **Decay channels:** |
|---|---|---|
| S-wave | $0^{++}$ | $\eta_c\eta_c$, $\boldsymbol{J/\psi J/\psi}$, $\chi_{c1}\eta_c$(P-wave), $J/\psi h_c(1P)$(P-wave), $J/\psi\psi(2S)$, $\chi_{c0}\chi_{c0}$ |
| S-wave | $1^{+-}$ | $\eta_c J/\psi$, $h_c\eta_c$(P-wave), $J/\psi\chi_{c1}$(P-wave), $\eta_c\psi'$, $h_c\chi_{c0}$ |
| S-wave | $2^{++}$ | $\boldsymbol{J/\psi J/\psi}$, $\eta_c\chi_{c1}$(P-wave), $\eta_c\chi_{c2}$(P-wave), $J/\psi h_c$(P-wave), $J/\psi\psi(2S)$, $\chi_{c0}\chi_{c2}$ |
| P-wave | $0^{-+}$ | $\boldsymbol{J/\psi J/\psi}$(P-wave), $\eta_c\chi_{c0}$, $J/\psi h_c$, $J/\psi\psi(2S)$(P-wave) |
| P-wave | $1^{-+}$ | $\boldsymbol{J/\psi J/\psi}$(P-wave) $J/\psi h_c$, $J/\psi\psi(2S)$(P-wave) |
| P-wave | $2^{-+}$ | $\boldsymbol{J/\psi J/\psi}$(P-wave), $\eta_c\chi_{c2}$, $J/\psi h_c$, $J/\psi\psi(2S)$(P-wave) |
| P-wave | $0^{--}$ | $\eta_c J/\psi$(P-wave), $J/\psi\chi_{c1}$, $\eta_c\psi(2S)$(P-wave) |
| P-wave | $1^{--}$ | $\eta_c J/\psi$(P-wave), $\eta_c h_c$, $J/\psi\chi_{c0}$, $J/\psi\chi_{c1}$, $J/\psi\chi_{c2}$, $\eta_c\psi'$(P-wave) |
| P-wave | $2^{--}$ | $\eta_c J/\psi$(P-wave), $J/\psi\chi_{c1}$, $J/\psi\chi_{c2}$, $\eta_c\psi'$(P-wave), $h_c\chi_{c0}$(P-wave) |
| P-wave | $3^{--}$ | $J/\psi\chi_{c2}$ |

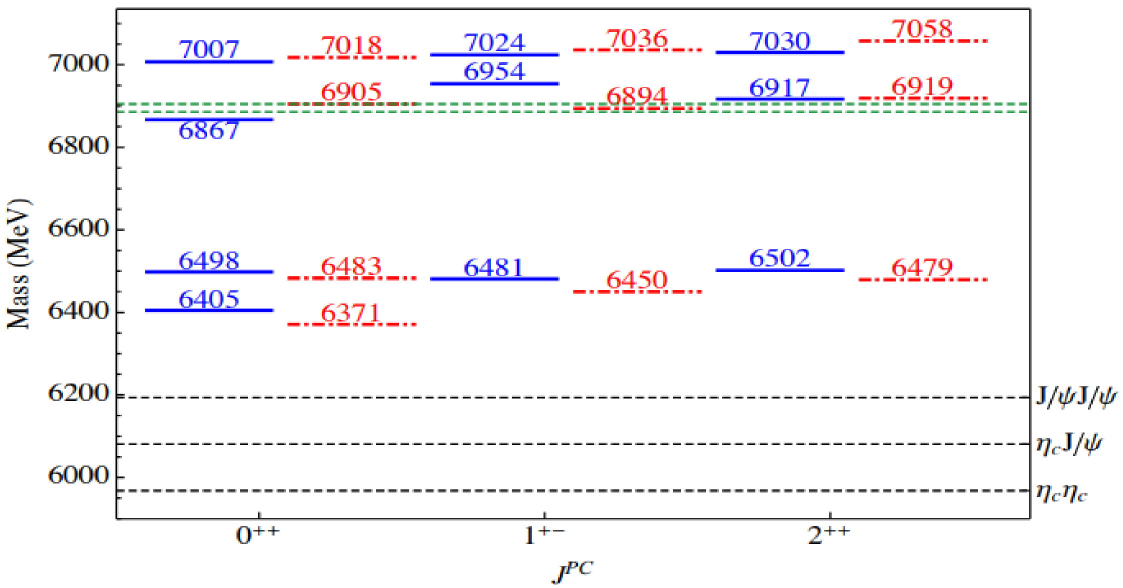


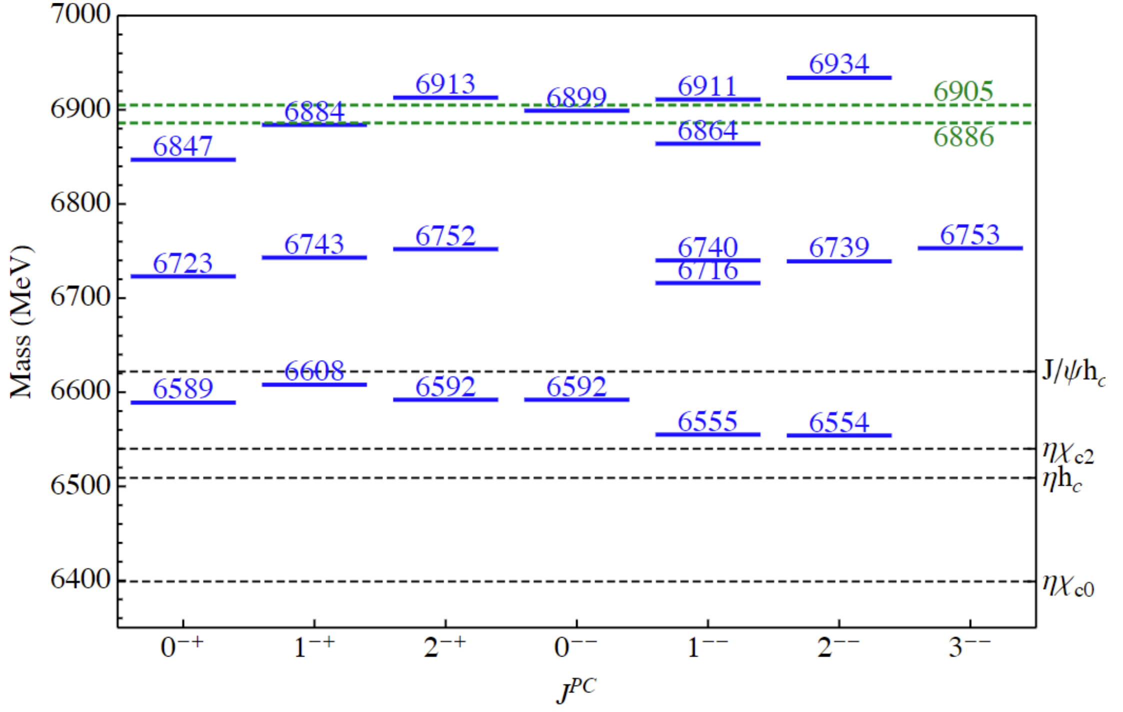

# Predictions of theoretical models

## Compact tetraquark

[10] Quark Confinement for Multi-Quark Systems -- Application to Fully-Charmed Tetraquarks [arxiv:2307.04310]

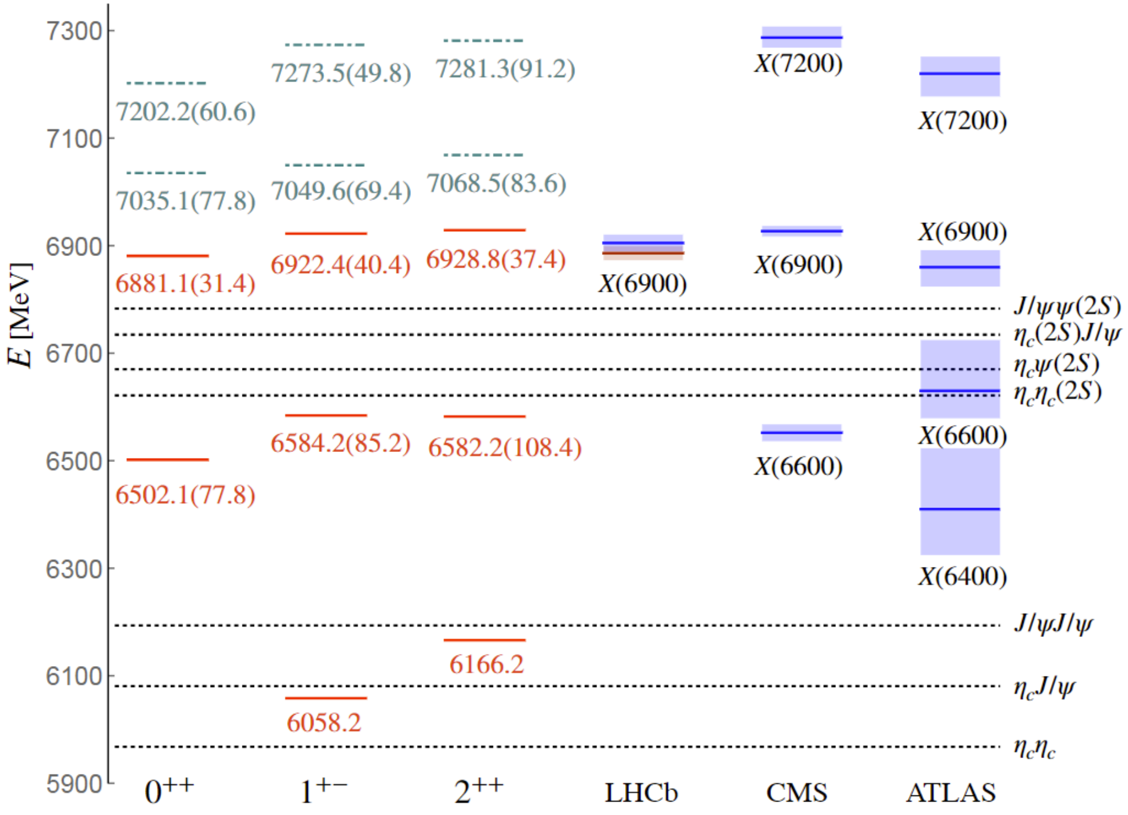


A new color basis system and confinement mechanism for multi-quark systems are proposed

- States at **6502, 6881, 7035** and **7202** are predicted for **0++**
- **Bound states are predicted**

## Dynamic mechanisms

Compact or molecular structures with **channel rescattering interactions**. Different charmonium pairs directly produced by pp collision may transit into the final state of J/ψJ/ψ.

[11] Some remarks on X(6900) [arxiv:2011.04347] *LHCb data

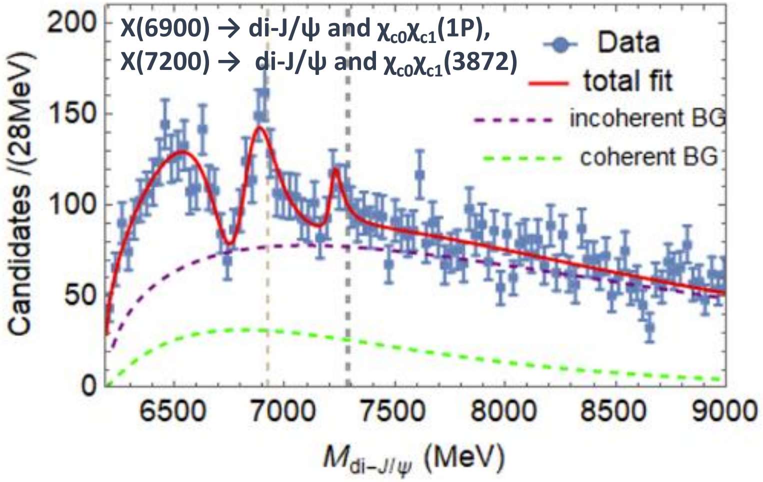


Table I. Involved $S$-wave couple channels except di-$J/\psi$.

| $J^{PC}$ of di-$J/\psi$ | Couple channels of $X(6900)$ | Threshold (MeV) | Couple channels of $X(7200)$ |
|---|---|---|---|
| $0^{++}$ | $J/\psi-\psi(2S)$<br>$J/\psi-\psi(3770)$ | 6783.0<br>6870.6 | $J/\psi-\psi(4160)$ |
| $2^{++}$ | $J/\psi-\psi(2S)$<br>$J/\psi-\psi(3770)$<br>$J/\psi-\psi_2(3823)$<br>$J/\psi-\psi_3(3842)$ | 6783.0<br>6870.6<br>6919.1<br>6939.6 | $J/\psi-\psi(4160)$ |

Table II. Involved $P$-wave couple channels except di-$J/\psi$.

| $J^{PC}$ of di-$J/\psi$ | Couple channels of $X(6900)$ | Threshold (MeV) | Couple channels of $X(7200)$ |
|---|---|---|---|
| $1^{-+}$<br>$(0,1,2)^{-+}$ | $\chi_{c0}-\chi_{c1}$<br>$J/\psi-\psi(3770)$ | 6925.4<br>6870.6 | $\chi_{c0}-\chi_{c1}(3872)$<br>$J/\psi-\psi(4160)$ |

# Predictions of difenitions cross-sections

[13] Fully charmed tetraquark production at the LHC experiments [arXiv:2409.12070]

For unpolarized T4c(0++, 1+−, 2++) models were predicted the $d\sigma/dp_T$ spectra in the kinematic ranges accessible at the ongoing LHC experiments. The state **$2^{++}$(2S)** of $T_{4c}$ is the best matching candidate for **X(6900)**.

TABLE I: Reduced cross-section $\overline{\sigma} = \sigma/\Phi$ at the proton-proton collision energy $\sqrt{S} = 13$ TeV for particular kinematic conditions. For the definition and typical values of $\Phi$, see Appendix A. The reduced cross-sections are calculated with CTEQ18 parametrization for the strong coupling and gluon density functions. The values are presented along with their uncertainties as follows: $\overline{\sigma} + \Delta\overline{\sigma}(\text{scale}) + \Delta\overline{\sigma}(\text{mass}) + \Delta\overline{\sigma}(\alpha^2)$.

| Final state | Kinematic region | | |
|---|---|---|---|
| | $2 < y < 5$, $5 < p_T(\text{GeV}) < 50$ (appr. corresponds to LHCb) | $\lvert y\rvert < 2$, $10 < p_T(\text{GeV}) < 100$ (accessible at CMS) | $\lvert y\rvert < 2$, $20 < p_T(\text{GeV}) < 100$ (accessible at ATLAS/CMS) |
| $0^{++}(nS) + g$ | $550\ ^{+300}_{-200}\ ^{+40}_{-30}\ ^{+30}_{-20}$ pb | $110\ ^{+70}_{-40}\ ^{+7}_{-3}\ ^{+11}_{-4}$ pb | $3.70\ ^{+2.40}_{-1.40}\ ^{+0.30}_{-0.40}\ ^{+0.30}_{-0.30}$ pb |
| $1^{+-}(nS) + g$ | $7.30\ ^{+2.60}_{-2.20}\ ^{+0.12}_{-0.02}$ pb | $0.90\ ^{+0.40}_{-0.30}\ ^{+0.07}_{-0.09}$ pb | $0.011\ ^{+0.006}_{-0.004}\ ^{+0.001}_{-0.002}$ pb |
| $2^{++}(nS) + g$ | $7500\ ^{+4300}_{-2900}\ ^{+600}_{-550}$ pb | $1690\ ^{+950}_{-600}\ ^{+40}_{-70}$ pb | $57\ ^{+38}_{-21}\ ^{+5}_{-6}$ pb |

TABLE III: Predicted parameters of $T_{4c}$ candidates for $X(6900)$. The values should be compared with Eq. (46).

| | $0^{++}(2S)$ | | $0'^{++}(2S)$ | | $2^{++}(2S)$ | |
|---|---|---|---|---|---|---|
| | Mass, MeV | $\Phi^{(0)}(2S)\cdot\text{Br}(T_{4c}(0^{++}))$ | Mass, MeV | $\Phi^{(0')}(2S)\cdot\text{Br}(T_{4c}(0^{++}))$ | Mass, MeV | $\Phi^{(2)}(2S)\cdot\text{Br}(T_{4c}(2^{++}))$ |
| Refs. [15, 26] | 6867 | $0.047\cdot10^{-3}$ | 7007 | $0.091\cdot10^{-3}$ | 6917 | $0.034\cdot10^{-3}$ |
| Refs. [15, 27] | 6849 | $0.059\cdot10^{-3}$ | 6940 | $0.070\cdot10^{-3}$ | 6948 | $0.109\cdot10^{-3}$ |

# Amplitude analysis. Decay kinematics of $X_{cc\bar{c}\bar{c}}$

Existing experimental studies provide measurements of mass and width of the new resonances: broad structure at 6600 MeV and narrow structures at 6900 and 7200 MeV. However, their **spin-parity properties** have to confirmed yet [5]. The amplitude analysis enables a more precise analysis of the properties of X(6900) and other signal states. We are working on **amplitude analysis** using the **Helicity amplitude formalism** of J/ψ meson pairs in the ATLAS data. This can allow to get **sensitivity to parameters** of exotic states X-6600, X-6900, X-7200.

$$M_{total} = \sum_{\substack{\lambda_{X0},\\ \lambda_{X1},\lambda_{X2},\\ \lambda_{\mu1},\lambda_{\mu2}}} \left| \sum_{\lambda_{\psi1},\lambda_{\psi2}} A_{di-J/\psi} \right|^2 + \sum_{\substack{\lambda_{X0'},\\ \lambda_{X1'},\lambda_{X3},\\ \lambda_{\mu3},\lambda_{\mu4}}} \left| \sum_{\lambda_{\psi3},\lambda_{\psi4}} A_{J/\psi-\psi(2S)} \right|^2 + \dots$$

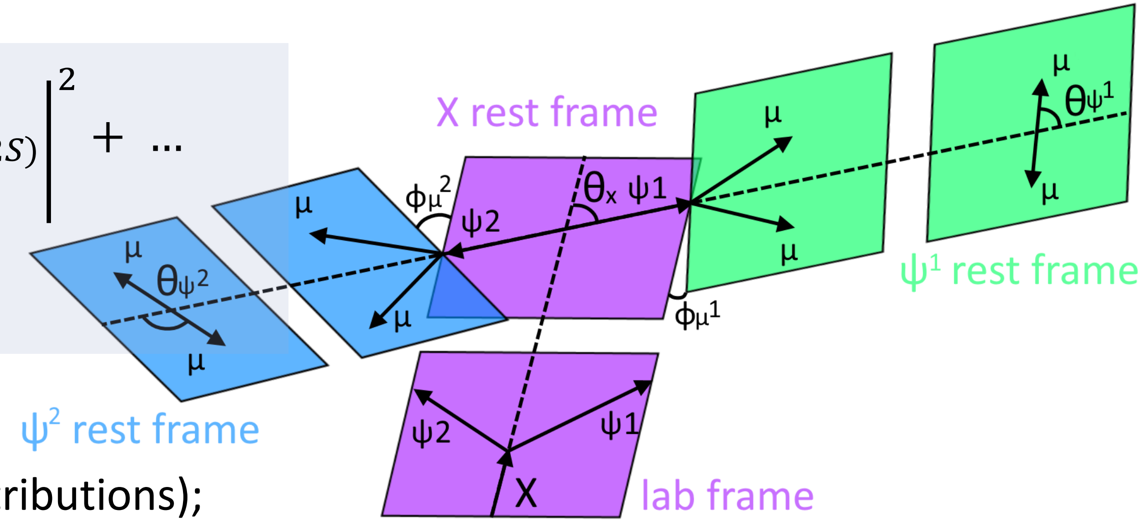


<u>Helicity formalism</u>:

- Allows for multidimensional fits (invariant mass and angular distributions);
- Gain sensitivity for spin-parity;
- Account interference effects between different amplitudes;
- Takes into account detector effects.

- Angular variables determining the kinematics of decay: $\theta_X, \phi_{\mu_1}, \theta_{\psi_1}, \phi_{\mu_2}, \theta_{\psi_2}$
- $\theta_X$ is the decay angle sensitive to $X$ spin

# Prediction of our model for the tetraquark spectrum

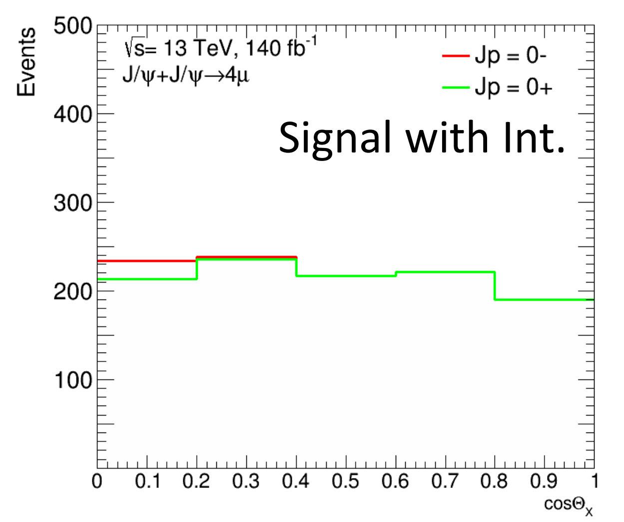


All resonances are assumed to have 0+ spin-parity.
Comparison to the **interference picture** derived from **CMS** data[2] shows similar amplitude structures near 6.9 GeV.

| | $BW_1(0^+)$ | $BW_2(0^+)$ | $BW_3(0^+)$ |
|---|---|---|---|
| **m, GeV** | 6.59 | 6.87 | 7.07 |
| **Γ, GeV** | 0.481 | 0.196 | 0.353 |

**J/ψ + J/ψ → 4μ**

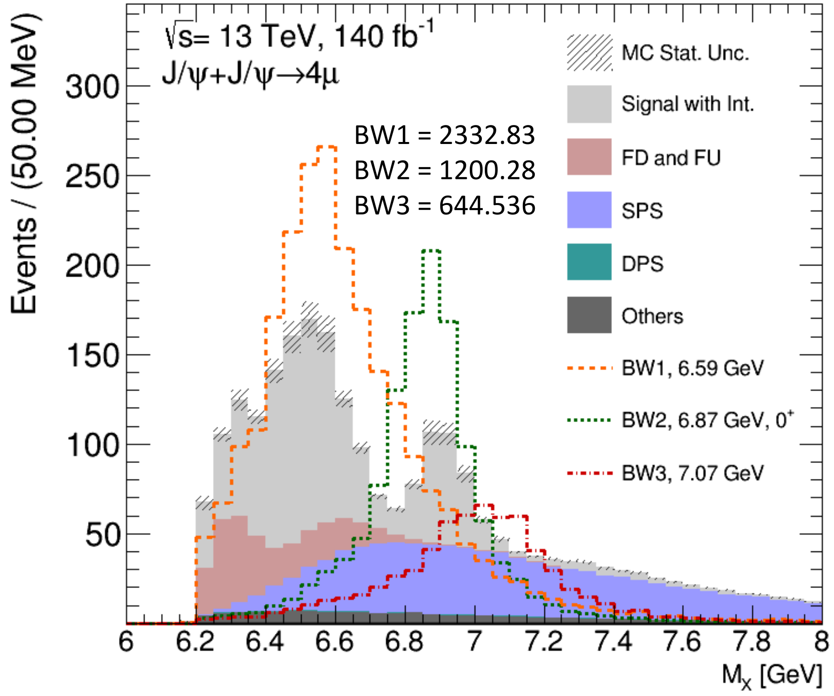


**J/ψ + ψ(2S) → 4μ**

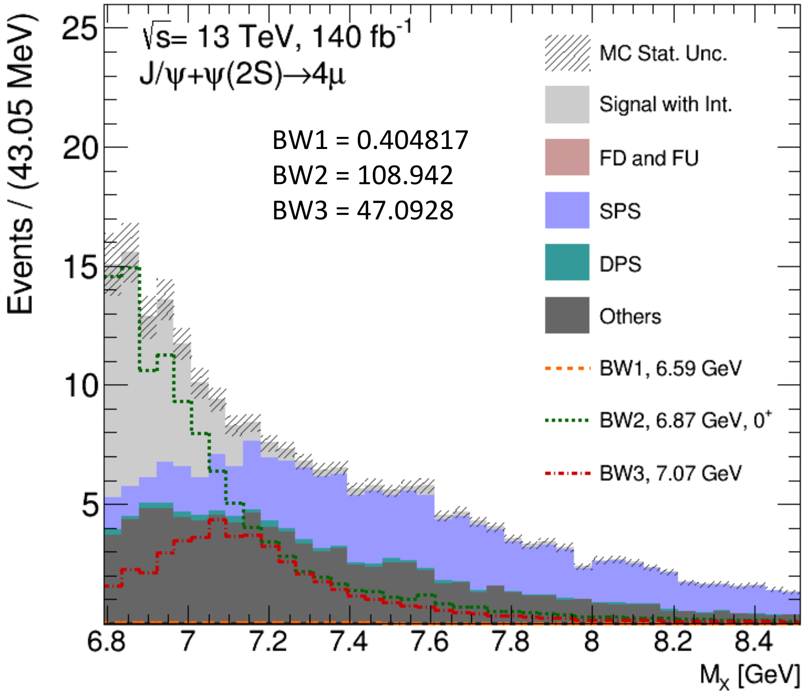


**J/ψ + ψ(2S) → 4μ + 2π**

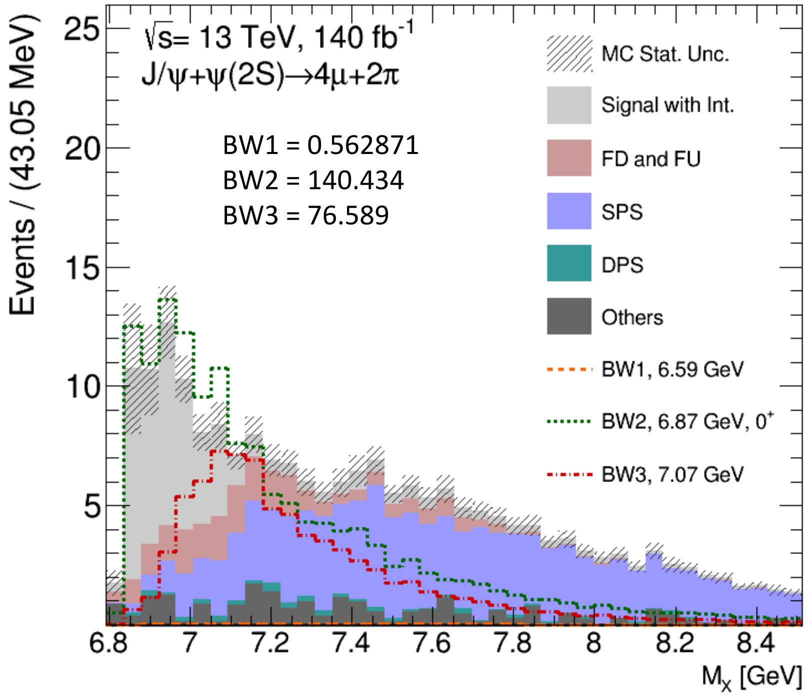

# Conclusion and outlook

- There are many experimental observations of excess mass of $T_{cc\bar{c}\bar{c}}$ , but the precise quantum characteristics have not been researched: LHCb, CMS, ATLAS. CMS compared models with different quantum numbers for J/ψ-J/ψ channel only. $J^p = 0^-$ is excluded for X(6900), preferred is $J^p = 2^+$. Low mass threshold effects need investigations in a complex analysis

- There are many theoretical models that predict different structure of the observed states: Compact tetraquark, Dynamic mechanisms, diquark-antidiquark, etc. Different models predict different decay channels and different spin-parities.

- Pt signal spectrum is sensitive to the mechanism of $T_{cc\bar{c}\bar{c}}$ production (SPS or DPS)

- Sensitivity to $J^P$ of $T_{cc\bar{c}\bar{c}}$ is possible via analysis of the angular distributions

- **The amplitude analysis method has been applied** to describe mass and angular spectra of the observed signals in J/ψ-J/ψ and J/ψ-ψ(2S) decay channels observed in ATLAS experimental data. All resonances are assumed to have 0+ spin-parity. Their masses are 6.59, 6.87 and 7.07 GeV. The parameters were extracted from a simultaneous fit to the di-J/ψ and J/ψ-ψ(2S) channels.

- Preliminary comparison to the **interference picture** derived from **CMS** data[2] shows similar amplitude structures near 6.9 GeV.

**Thank you for your attention**

# References


[1] Observation of structure in the J/ψ-pair mass spectrum [arXiv:2006.16957v2]

[2] Observation of an excess of di-charmonium events in the four-muon final state with the ATLAS detector [arXiv:2304.08962v2]

[3] New Structures in the J/ψJ/ψ Mass Spectrum in Proton-Proton Collisions at √s = 13 TeV [arXiv:2306.07164v2]

[4] On the mechanism of T4c(6900) tetraquark production [arXiv:2009.02100v1]

[5] Particle Data Group [et al.] Review of Particle Physics // DOI: 10.1103/PhysRevD.110.030001 (2024).

[6] CERN LHC Seminar: Symmetry properties of all-charm tetraquarks with CMS (8 April 2025) [https://indico.cern.ch/event/1533044/]

[7] Observation of X(6900) and evidence of X(7100) in the psi(2S)Jpsi to 4mu mass spectrum in pp collisions at CMS (2025)

[8] Spin and symmetry properties of all-charm tetraquarks (2025)

[9] Higher fully-charmed tetraquarks: Radial excitations and P-wave states [arXiv:2105.13109]

[10] Quark Confinement for Multi-Quark Systems -- Application to Fully-Charmed Tetraquarks [arxiv:2307.04310]

[11] Some remarks on X(6900) [arxiv:2011.04347]

[12] Fully-heavy tetraquarks in the vacuum and in a hot environment [arxiv:2503.12160]

[13] Fully charmed tetraquark production at the LHC experiments [arXiv:2409.12070]

[14] Experimental Road to a Charming Family of Tetraquarks ... and Beyond [arXiv:2410.11210]

# The latest experimental observation. ATLAS

[2] Observation of an excess of di-charmonium events in the four-muon final state with the ATLAS detector [arXiv:2304.08962v2]

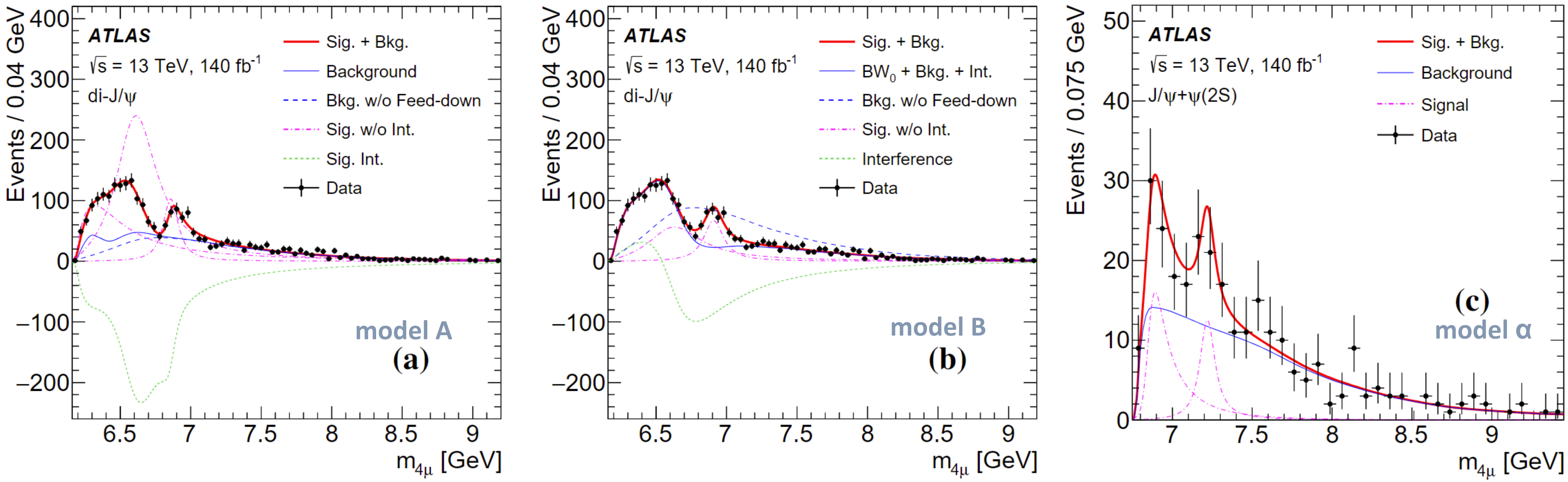


- **Model A**: interference of three states with each other;
- **Model B**: threshold structures interferes with SPS, and the second is added without interference;
- **Model α**: mass at 6.9 is fixed on model A, and the state at 7.2 is added without interference.

The mass of the third resonance, $m2$, is consistent with the LHCb mass.

| | | $BW_0$ | $BW_1$ | $BW_2$ |
|---|---|---|---|---|
| model A | m, GeV | 6.41 | 6.63 | 6.86 |
| | Γ, GeV | 0.59 | 0.35 | 0.11 |
| model B | m, GeV | 6.65 | - | 6.91 |
| | Γ, GeV | 0.44 | - | 0.15 |

| | $BW_3$ |
|---|---|
| model α | 7.22 |
| | 0.09 |
| model β | 6.96 |
| | 0.51 |

# Amplitude analysis. Decay kinematics of $X_{cc\bar{c}\bar{c}}$

$$M_{total} = \sum_{\lambda_X} \Big| \sum_{i} \sum_{\substack{\lambda_{\psi 1},\lambda_{\psi 2},\\ \Delta\lambda_{\mu 1},\Delta\lambda_{\mu 2}}} A_{X\to\psi_1\psi_2} \cdot A_{\psi_1\to 4\mu} \cdot A_{\psi_2\to 4\mu} \Big|^2$$

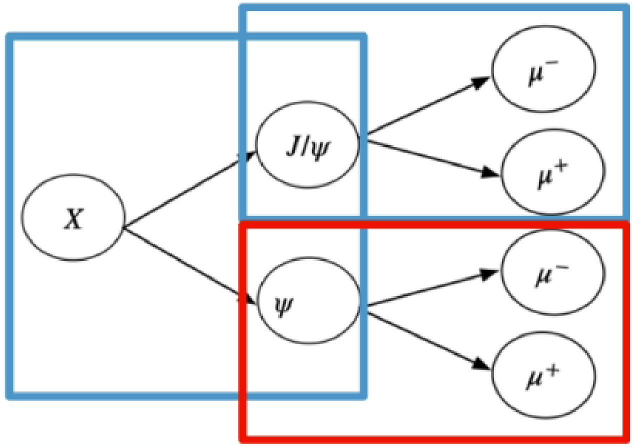


The amplitude $A_{X\to\psi_1\psi_2}$ is described by helical amplitude $H^{X\to\psi\psi}_{\lambda_\psi,\Delta\lambda_\mu}$ (which contains fit parameters), Breit-Wigner function BW with the resonance pole mass $M_0^X$ and width $\Gamma_0^X$, Blatt-Weisskopf factor $B'_L$(responsible for suppression of amplitude components with higher orbital momenta L), and Wigner D-matrices of X, ψ1 and ψ2:

$$A_{X\to\psi_1\psi_2} = H^{X\to\psi_1\psi_2}_{\lambda_{\psi 1},\lambda_{\psi 2}} \cdot BW(m_{\psi_1\psi_2}|M_0^X,\Gamma_0^X) \cdot B'_L(q,q_0,d) \cdot \left(\frac{q}{M_0^X}\right)^L \cdot D^{J_X}_{\lambda_X,\lambda_{\psi 1}-\lambda_{\psi 2}}(0,\theta_X,0)^*$$

$$A_{\psi_j\to 4\mu} = D^1_{\lambda_{\psi j},\Delta\lambda_{\mu j}}(\varphi_{\psi_1},\theta_{\psi_1},0)^*$$

In our notations of $B'_L$ arguments, $q$ is $\psi$ momentum in the $X$ reference frame, $q_0$ is the same momentum at $m_{\psi_1\psi_2} = M_0^X$, and $d$ is a scale parameter of $T_{cc\bar{c}\bar{c}}$.

$$\mathcal{H}^{A\to BC}_{\lambda_B,\lambda_C} = \sum_L \sum_S (-1)^{J_B-J_C+L-S+2\lambda_B-2\lambda_C} \sqrt{(2L+1)(2S+1)} B_{LS} \times \begin{pmatrix} J_B & J_C & S \\ \lambda_B & -\lambda_C & \lambda_C-\lambda_B \end{pmatrix} \begin{pmatrix} L & S & J_A \\ 0 & \lambda_B-\lambda_C & \lambda_C-\lambda_B \end{pmatrix}$$

# Predictions of theoretical models

[12] Fully-heavy tetraquarks in the vacuum and in a hot environment [arxiv:2503.12160]

The structures **X(6600)**, **X(6900)** and **X(7200)** are the radially-excited **$T_{4c}(n^1S_0)$** configurations with n = 2, 3, 4.
However, one should notice that there is not yeta definite theoretical description for the experimental data.

| $T_{4Q}$ | $n^{2s+1}l_j$ | $M$ [GeV] | $M_{NIF}^{(Exp)}$ [GeV] [3] | $M_{IF}^{(Exp)}$ [GeV] [3] |
|---|---|---|---|---|
| $T_{4c}$ | $2^1S_0$ | $6.55988 \pm 0.117449$ | $6.552 \pm 0.010 \pm 0.012$ | $6.638^{+0.043+0.016}_{-0.038-0.031}$ |
| $T_{4c}$ | $3^1S_0$ | $6.91895 \pm 0.116399$ | $6.927 \pm 0.009 \pm 0.004$ | $6.847^{+0.044+0.048}_{-0.028-0.020}$ |
| $T_{4c}$ | $4^1S_0$ | $7.20517 \pm 0.11512$ | $7.287^{+0.020}_{-0.018} \pm 0.005$ | $7.134^{+0.048+0.041}_{-0.025-0.015}$ |

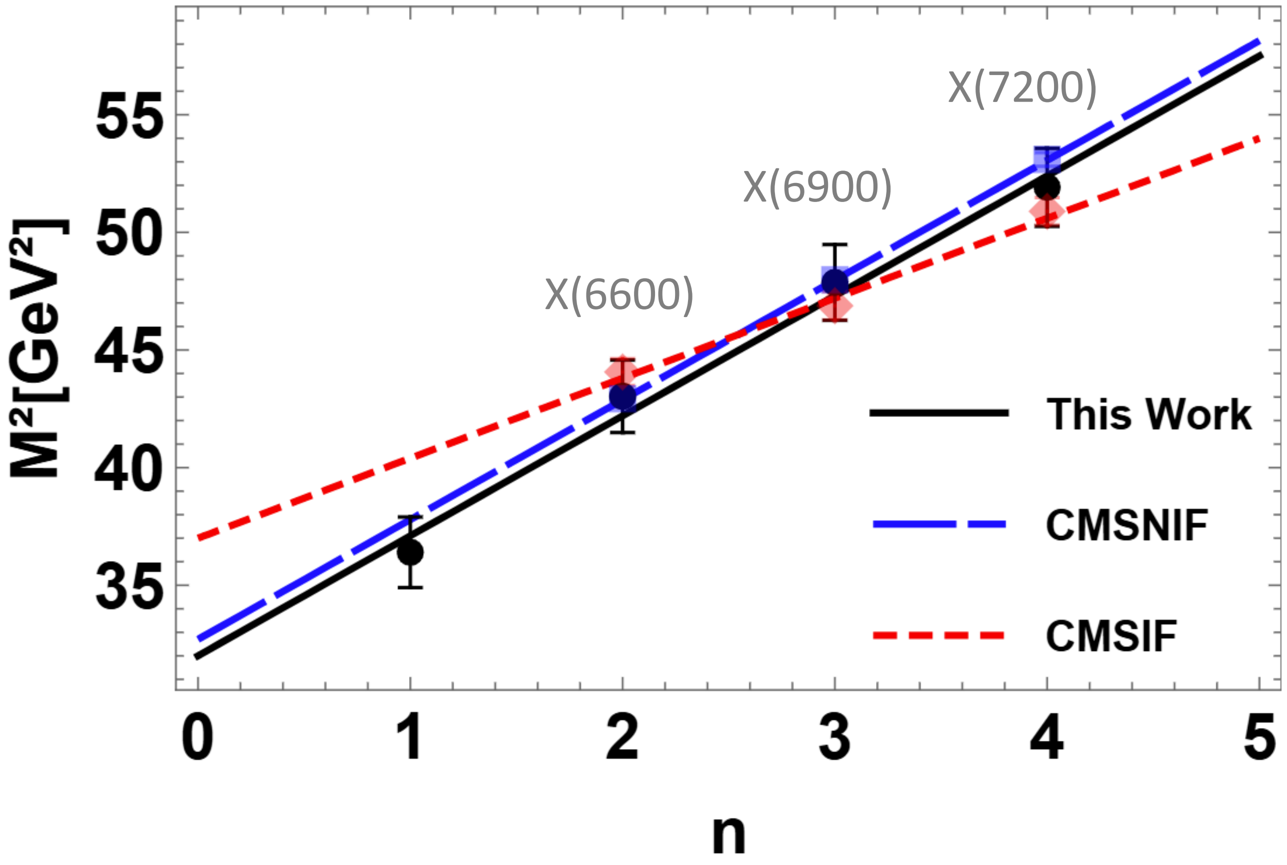


[13] Fully charmed tetraquark production at the LHC experiments [arXiv:2409.12070]

In the previous study proposed the interpretation of **X(6900)** as a **T4c[$2^{++}$(2S)]**.

[14] Experimental Road to a Charming Family of Tetraquarks ... and Beyond [arXiv:2410.11210]

While in another study, the triplet masses is interpreted by a typical Regge trajectory of radial excitations, where the **X(6900)** is a **n = 3** radially excited state, as in [12].

# Predictions of theoretical models. Dynamic mechanisms

Compact or molecular structures with **channel rescattering interactions**.

[11] Some remarks on X(6900) [arxiv:2011.04347] *LHCb data

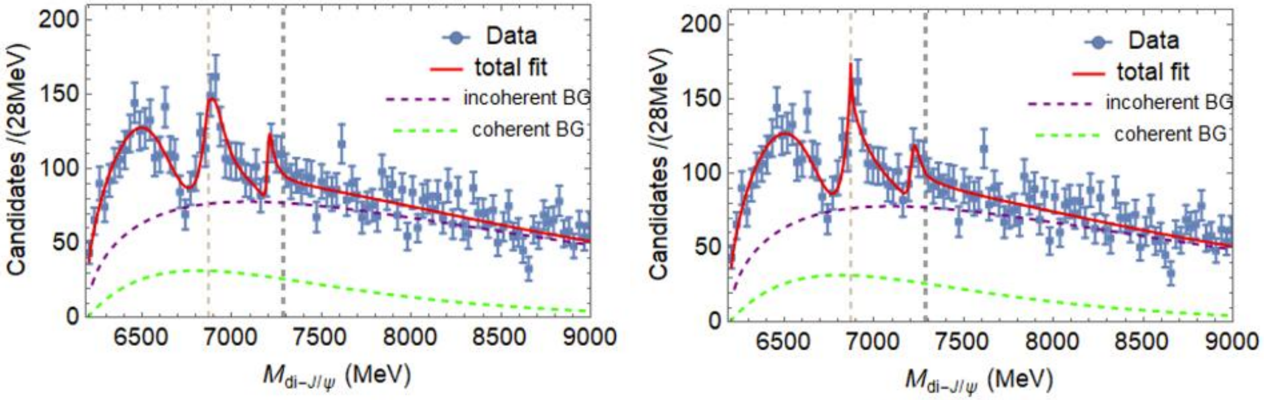


(a) Solution I (b) Solution II

*Figure 1.*
Fit projections of two solutions for the S−S couplings in Case I with the X(6900) → J/ψJ/ψ and J/ψψ(3770),
and X(7200)→J/ψJ/ψ and J/ψψ(4160) couples.

The dots with error bars are the LHCb data [6], the red lines are the best fit, the green dashed lines show the coherent BG, the purple dashed lines are the contribution of the incoherent BG, and the vertical lines indicate the corresponding mass thresholds of X(6900) and X(7200).

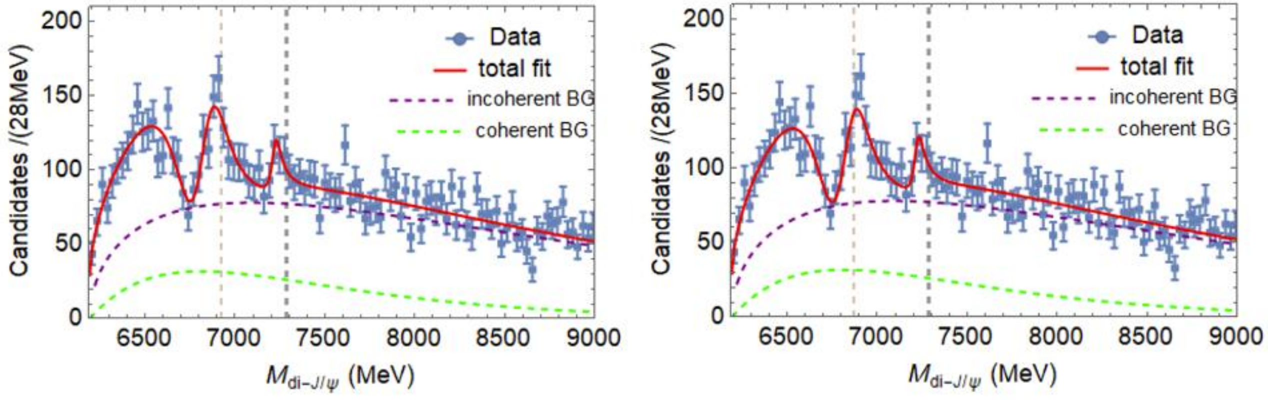


(a) Case I (b) Case II

*Figure 2.*
Fit projections for the P−P couplings, where Fig. (a) shows X(6900) decaying to J/ψJ/ψ and χc0χc1, and X(7200) to J/ψJ/ψ and χc0χc1(3872), and Fig. (b) illustrates X(6900) → J/ψJ/ψ and J/ψψ(3770), X(7200)→J/ψJ/ψ and J/ψψ(4160). Here, the descriptions of the components of the figures are similar to those of Fig. 1.

Table III. Parameters for the involved charmonium states [20].

| | $J/\psi$ | $\chi_{c0}$ | $\chi_{c1}$ | $\psi(2S)$ | $\psi(3770)$ | $\psi_2(3823)$ | $\psi_3(3842)$ | $\chi_{c1}(3872)$ | $\psi(4160)$ |
|---|---|---|---|---|---|---|---|---|---|
| $J^{PC}$ | $1^{--}$ | $0^{++}$ | $1^{++}$ | $1^{--}$ | $1^{--}$ | $2^{--}$ | $3^{--}$ | $1^{++}$ | $1^{--}$ |
| mass (MeV) | 3096.9 | 3414.7 | 3510.7 | 3686.1 | 3773.7 | 3822.2 | 3842.7 | 3871.7 | 4191.0 |
| $n^{2S+1}L_J$ | $1^3S_1$ | $1^3P_0$ | $1^3P_1$ | $2^3S_1$ | $1^3D_1$ | $1^3D_2$ | $1^3D_3$ | $2^3P_1$ [21] | $2^3D_1$ |

# Predictions of theoretical models. Dynamic mechanisms

[12] Improved understanding of the peaking phenomenon existing in the new di-J/ψ invariant mass spectrum from the CMS Collaboration [arXiv:2207.04893v3]

The excess di-J/ψ may be due to the transition of different charmonium pairs to the final state J/ψ-J/ψ.

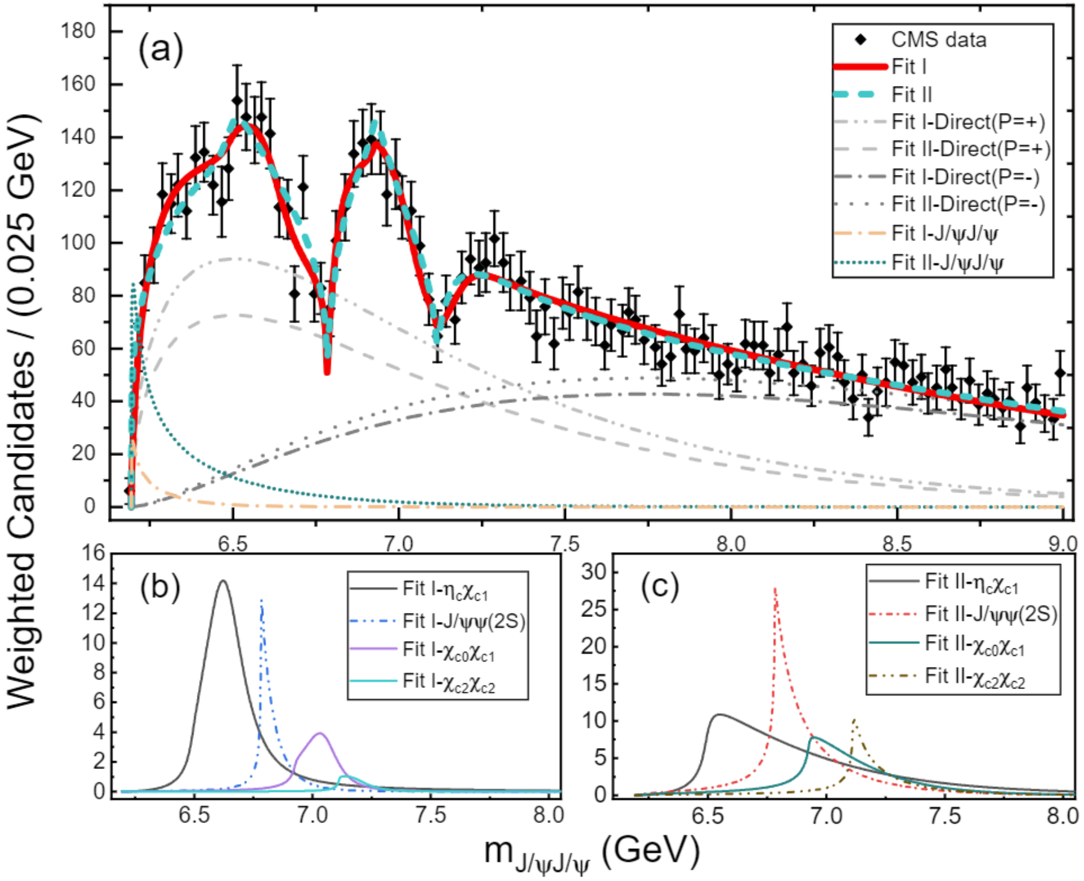


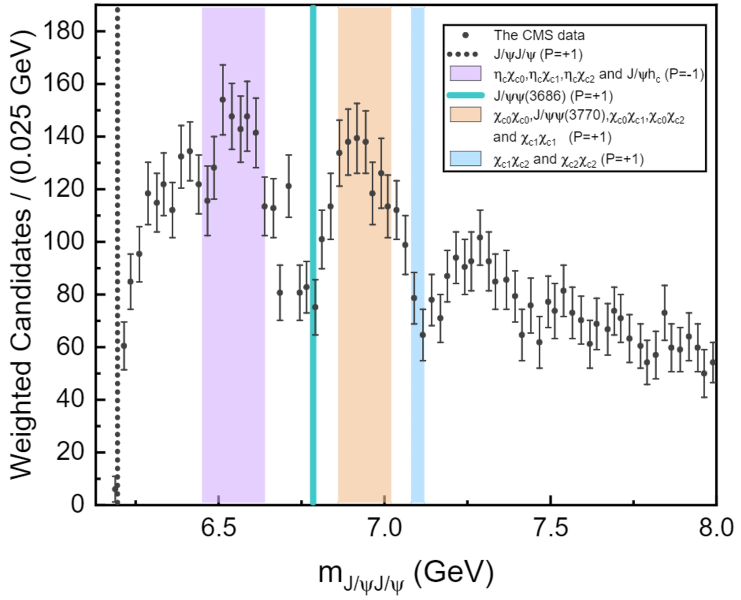


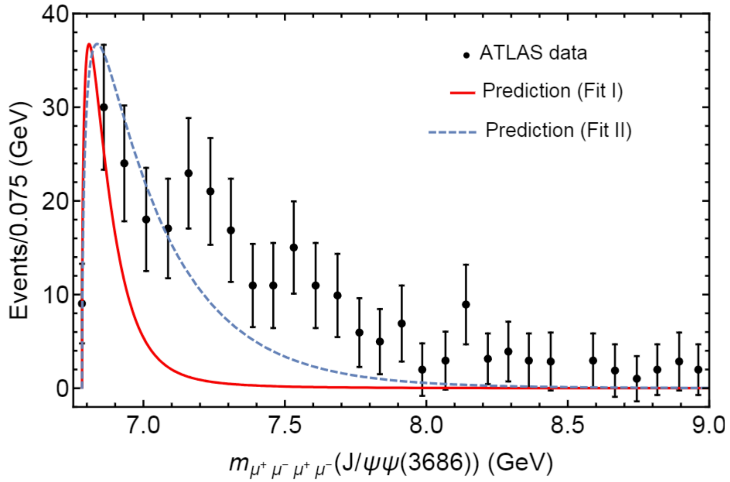


The complete theoretical fit to the invariant mass distribution of J/ψ pair measured by the CMS Collaboration within an extended dynamical mechanism. Four channel interaction included: **$\eta_c\chi_{c1}$, $J/\psi\psi(2S)$, $\chi_{c0}\chi_{c1}$, $\chi_{c2}\chi_{c2}$**

# Predictions of theoretical models. Hadronic molecules

Theories of hadronic molecules are also not excluded

[13] Hadronic $\eta_c\eta_c$, $\chi_{c0}\chi_{c0}$ molecules [arXiv:2305.03696]

The observed signal X(6200) can be interpreted as hadronic scalar molecule $\boldsymbol{\eta_c\eta_c}$, and X(6900) as an another scalar tetraquark molecule of $\boldsymbol{\chi_{c0}\chi_{c0}}$

[14] The X(6900) peak could be a molecular state [arXiv:2302.04150]

The X(6900) peak could be a molecular state of **J/ψψ(3770)** or $\boldsymbol{\chi_{c0}\chi_c}$

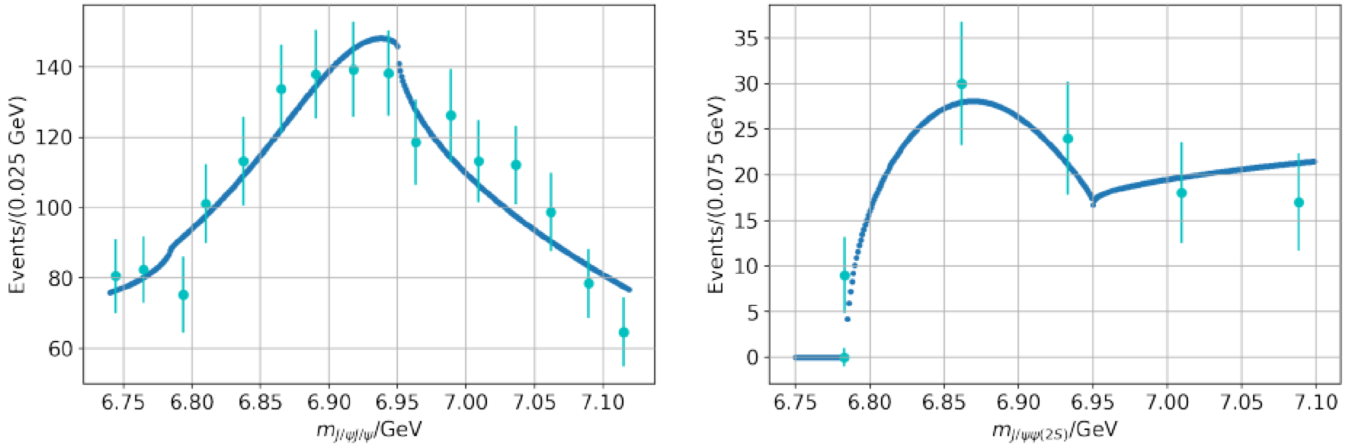


Figure: Fit to the invariant mass spectrum, for the molecule solution.

*The CMS data [8a]

[15] Resonance X(7300): excited 2S tetraquark or hadronic molecule $\chi_{c1}\,\chi_{c1}$? [arXiv:2307.01857v1]

In accordance to these results, both the excited tetraquark and hadronic molecule may be considered as candidates to the resonance X(7300). Detailed analysis, however, demonstrates that the preferable model for X(7300) is an admixture of the molecule M and sizeable part of $X^*_{4c}$ (first radial excitation $X^*_{4c}$ of the fully charmed diquark-antidiquark state $X_{4c}$)

# Amplitude analysis. Decay kinematics of $X_{cc\bar{c}\bar{c}}$ with $4\mu$ in final state

$$M_{total} = \sum_{\substack{\lambda_{X0},\\ \lambda_{X1},\lambda_{X2},\\ \lambda_{\mu1},\lambda_{\mu2}}} \left| \sum_{\lambda_{\psi1},\lambda_{\psi2}} A_{di-J/\psi} \right|^2 + \sum_{\substack{\lambda_{X0'},\\ \lambda_{X1'},\lambda_{X3},\\ \lambda_{\mu3},\lambda_{\mu4}}} \left| \sum_{\lambda_{\psi3},\lambda_{\psi4}} A_{J/\psi-\psi(2S)} \right|^2$$

- Angular variables determining the kinematics of decay: $\theta_X, \phi_{\mu_1}, \theta_{\psi_1}, \phi_{\mu_2}, \theta_{\psi_2}$
- $\theta_X$ is the decay angle sensitive to $X$ spin

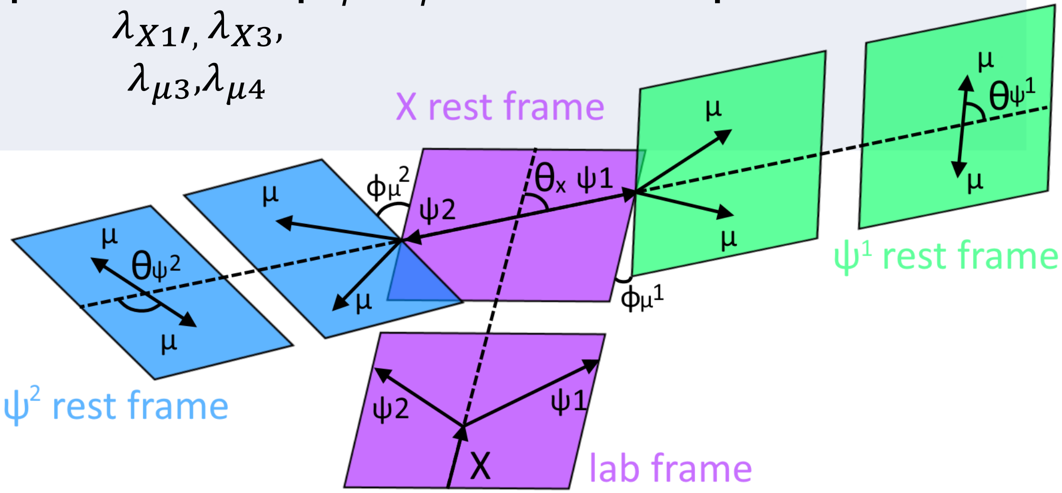


$$A = A_{X0} + A_{X1} + A_{X2} + \ \dots$$
$$A_{Xstate} = A_X * A_{J/\psi_1} * A_{J/\psi_2}$$

add up coherently

$$A_X(\lambda_X, \lambda_{\psi_1}, \lambda_{\psi_2}) = H^{X\to J/\psi\, J/\psi}_{\lambda_\psi,\Delta\lambda_\mu} D^{J_X}_{\lambda_X,\lambda_{\psi_1}-\lambda_{\psi_2}}(\phi_\psi, \theta_\psi, 0) * R_X(m_{J/\psi\, J/\psi})$$

$X \to J/\psi\ J/\psi$

$$A_{J/\psi}(\lambda_\psi, \Delta\lambda_\mu) = D^1_{\lambda_\psi,\Delta\lambda_\mu}(\phi_\psi, \theta_\psi, 0)^*$$

$J/\psi_i \to \mu^+\mu^-$

# Amplitude analysis. Decay kinematics of $X_{cc\bar{c}\bar{c}}$ with $4\mu$ in final state

$$\mathcal{H}^{A\to BC}_{\lambda_B,\lambda_C} = \sum_L \sum_S (-1)^{J_B-J_C+L-S+2\lambda_B-2\lambda_C} \sqrt{(2L+1)(2S+1)} B_{LS} \times \begin{pmatrix} J_B & J_C & S \\ \lambda_B & -\lambda_C & \lambda_C-\lambda_B \end{pmatrix} \begin{pmatrix} L & S & J_A \\ 0 & \lambda_B-\lambda_C & \lambda_C-\lambda_B \end{pmatrix}$$

$$J_\psi = 1,$$
$$P_\psi = -1,$$
$$\vec{S} = \vec{J}_\psi + \vec{J}_\psi = \vec{0}, \vec{1}, \vec{2},$$
$$\vec{P}_X = (P_\psi)(P_\psi)(-1)^L = (-1)(-1)(-1)^L,$$
$$\vec{L} = \vec{J}_X - \vec{S},$$

3j-symbol calculator: https://www-stone.ch.cam.ac.uk/wigner.shtml

| $J_X^P$ | $H_{\lambda_{\psi_1},\lambda_{\psi_2}}$ | $H_{-\lambda_{\psi_1},-\lambda_{\psi_2}}$ | Явное выражение при заданной спин-четности |
|---|---|---|---|
| | $H_{0,0}$ | | $-\sqrt{1/3}B_{00} + \sqrt{2/3}B_{22}$ |
| | $H_{0,+1}$ | $H_{0,-1}$ | 0 |
| $0^+$ | $H_{+1,0}$ | $H_{-1,0}$ | 0 |
| | $H_{+1,+1}$ | $H_{-1,-1}$ | $\sqrt{1/3}B_{00} + \sqrt{1/6}B_{22}$ |
| | $H_{+1,-1}$ | $H_{-1,+1}$ | 0 |

$$A = A_{X0} + A_{X1} + A_{X2} + \ ...$$

add up coherently

$$A_{Xstate} = A_X * A_{J/\psi_1} * A_{J/\psi_2}$$

$$A_X(\lambda_X, \lambda_{\psi_1}, \lambda_{\psi_2}) = H^{X\to J/\psi\, J/\psi}_{\lambda_\psi,\Delta\lambda_\mu} D^{J_X}_{\lambda_X,\lambda_{\psi_1}-\lambda_{\psi_2}}(\phi_\psi, \theta_\psi, 0) * R_X(m_{J/\psi\, J/\psi})$$

$X \to J/\psi\ J/\psi$

$$A_{J/\psi}(\lambda_\psi, \Delta\lambda_\mu) = D^1_{\lambda_\psi,\Delta\lambda_\mu}(\phi_\psi, \theta_\psi, 0)^*$$

$J/\psi_i \to \mu^+\mu^-$

# Amplitude analysis. Decay kinematics of $X_{cc\bar{c}\bar{c}}$ with $4\mu$ in final state

$$R_X(m_{\psi\psi}) = BW(m_{\psi\psi}|M_0^X, \Gamma_0^X) B'_{L_\psi}(q, q_0, d) \left(\frac{q}{M_0^X}\right)^{L_\psi}$$

$$BW(m|M_0, \Gamma_0) = \frac{1}{M_0^2 - m^2 - iM_0\Gamma(m)},$$

$$\Gamma(m) = \Gamma_0 \left(\frac{q}{q_0}\right)^{2L_\psi+1} \frac{M_0}{m} B'_{L_\psi}(q, q_0, d)^2.$$

$$B'_0(p, p_0, d) = 1$$

$$B'_1(p, p_0, d) = \sqrt{\frac{1+(p_0 d)^2}{1+(pd)^2}}$$

$$B'_2(p, p_0, d) = \sqrt{\frac{9+3(p_0 d)^2+(p_0 d)^4}{9+3(pd)^2+(pd)^4}}$$

$$B'_3(p, p_0, d) = \sqrt{\frac{225+45(p_0 d)^2+6(p_0 d)^4+(p_0 d)^6}{225+45(pd)^2+6(pd)^4+(pd)^6}}$$

The **Wigner D-matrix** is a unitary square matrix of dimension 2*j* + 1 in this spherical basis with elements

$$D^j_{m'm}(\alpha, \beta, \gamma) \equiv \langle jm'|\mathcal{R}(\alpha, \beta, \gamma)|jm\rangle = e^{-im'\alpha} d^j_{m'm}(\beta) e^{-im\gamma}$$

$$d^j_{m'm}(\beta) = [(j+m')!(j-m')!(j+m)!(j-m)!]^{\frac{1}{2}} \sum_{s=s_{\min}}^{s_{\max}} \left[\frac{(-1)^{m'-m+s}\left(\cos\frac{\beta}{2}\right)^{2j+m-m'-2s}\left(\sin\frac{\beta}{2}\right)^{m'-m+2s}}{(j+m-s)!s!(m'-m+s)!(j-m'-s)!}\right]$$

$$A = A_{X0} + A_{X1} + A_{X2} + \ \ldots$$

add up coherently

$$A_{Xstate} = A_X * A_{J/\psi_1} * A_{J/\psi_2}$$

$$A_X(\lambda_X, \lambda_{\psi_1}, \lambda_{\psi_2}) = H^{X\to J/\psi\, J/\psi}_{\lambda_\psi, \Delta\lambda_\mu} D^{J_X}_{\lambda_X, \lambda_{\psi_1}-\lambda_{\psi_2}}(\phi_\psi, \theta_\psi, 0) * R_X(m_{J/\psi\, J/\psi})$$

$X \to J/\psi\ J/\psi$

$$A_{J/\psi}(\lambda_\psi, \Delta\lambda_\mu) = D^1_{\lambda_\psi, \Delta\lambda_\mu}(\phi_\psi, \theta_\psi, 0)^*$$

$J/\psi_i \to \mu^+\mu^-$